

## Supporting Information

### Color tuning of intrinsic white-light emission in anthracene-linker coordination networks

Chengfeng Yu,<sup>a</sup> Xiaoling Wang,<sup>a</sup> Ting Wu,<sup>a</sup> Xiangwei Gu,<sup>a</sup> Wei Huang<sup>a\*</sup>, Alexander M. Kirillov,<sup>b,c</sup> and Dayu Wu<sup>a\*</sup>

<sup>a</sup>Jiangsu Key Laboratory of Advanced Catalytic Materials and Technology, Advanced Catalysis & Green Manufacturing Collaborative Innovation Center, School of Petrochemical Engineering, Changzhou University, Changzhou, Jiangsu 213164, China.

<sup>b</sup>Centro de Química Estrutural and Departamento de Engenharia Química, Instituto Superior Técnico, Universidade de Lisboa, Av. Rovisco Pais, 1049-001 Lisboa, Portugal.

<sup>c</sup>Research Institute of Chemistry, Peoples' Friendship University of Russia (RUDN University), 6 Miklukho-Maklaya st., Moscow, 117198, Russia.

### Table of Contents

**Table S1** Partial bond length (Å) and bond angle (°) in the crystal structure of **1** and **2**.

**Table S2** H-bond distances (Å) and angles (°) in **1** and **2**.

**Fig. S1** FT-IR spectra of ligands, **1** and **2**.

**Fig. S2** Thermogravimetric curves of **1** and **2**.

**Fig. S3** A schematic assembly process of **2** and its structural representation.

**Fig. S4** Solid-state UV-Vis absorption spectra of **1** and **2**.

**Fig. S5** Solid-state emission spectra of **1** and organic ligands.

**Fig. S6** Concentration-dependent emission spectra of **bima** ligand in MeOH.

**Fig. S7** (a) Solid-state emission spectra of **2** at different excitation wavelengths at room temperature, (b) Temperature-dependent emission spectra of **2**. (c) Changes in HE and LE of **2** at different temperatures. (d) CIE coordinates of the emission spectrum of **2** at different temperatures.

**Fig. S8** Changes in the emission spectra and CIE coordinates of **2** before and after grinding.

**Fig. S9** Powder X-ray diffraction patterns of **1** (top) and **2** (bottom) before and after grinding.

**Synthesis of 9,10-bis(imidazole-1-methyl)anthracene (bima).** A mixture of imidazole (3.4 g, 50 mmol), NaOH (2.0 g, 50 mmol) and DMF (80 mL) was heated at 60°C for 1 hour, then 9,10-bis (bromomethyl) anthracene (9.1 g, 25 mmol) was added. The reaction mixture was kept at 80 °C for 12 hours and was then poured into 200 mL of ice water. A brown residue was obtained after filtration, which was dissolved in 100 mL of concentrated hydrochloric acid and filtered. The resulting solution was neutralized with NaOH solution and precipitation occurred. The yellow precipitate was filtered and washed several times with water, and dried under vacuum overnight (yield: 74%). <sup>1</sup>H NMR (400 MHz, DMSO) δ 8.63 (dt, J = 24.5, 12.3 Hz, 2H), 7.70 (dt, J = 18.4, 15.4 Hz, 3H), 6.87 (d, J = 63.0 Hz, 2H), 6.29 (d, J = 16.2 Hz, 2H).

**Table S1** Partial bond length (Å) and bond angle (°) in the crystal structure of **1** and **2**.

<b>1</b>			
Zn1–N2	2.012(2)	Zn1–N4	2.022(2)
Zn1–O2	1.968(2)	Zn1–Cl1	2.2554(8)
N4–Zn1–N2	105.73(9)	O2–Zn1–Cl1	113.28(6)
N4–Zn1–O2	104.39(9)	N2–Zn1–Cl1	104.21(7)
N2–Zn1–O2	121.69(9)	N4–Zn1–Cl1	106.48(7)
<b>2</b>			
Zn01–N003	2.004(3)	Zn01–O004	1.937(3)
Zn01–N003	2.004(3)	Zn01–O004	1.937(3)
O004–Zn01–O004	102.08(19)	N003–Zn01–N003	110.13(16)
O004–Zn01–N003	108.78(12)	O004–Zn01–N003	113.46(12)
O004–Zn01–N003	108.78(12)	O004–Zn01–N003	113.46(12)

**Table S2** H-bond distances (Å) and angles (°) in **1** and **2**.

D–H···A	d(D–H)	d(H···A)	d(D···A)	< DHA
<b>1</b>				
Intramolecular hydrogen bonding				
C11–H11···O1	0.9500	2.2094(37)	2.8771(39)	126.405°
C21–H21···O1	0.9500	2.6188(41)	3.1581(41)	116.443°
<b>2</b>				
Intramolecular hydrogen bonding				
C00C–H00d···O00A	0.9495	2.5788(47)	3.2947(47)	132.420°
C00B–H00c···O00A	0.9503	2.6784(51)	3.4034(51)	133.541°
Intermolecular hydrogen bonding				
C009–H009···O00A	0.9501	2.7725(53)	3.5378(53)	138.179°
C008–H00b···O00A	0.9899	2.4547(51)	3.4358(50)	170.900°
C00H–H00i···O00A	0.9499	3.0269(55)	3.5743(57)	118.132°

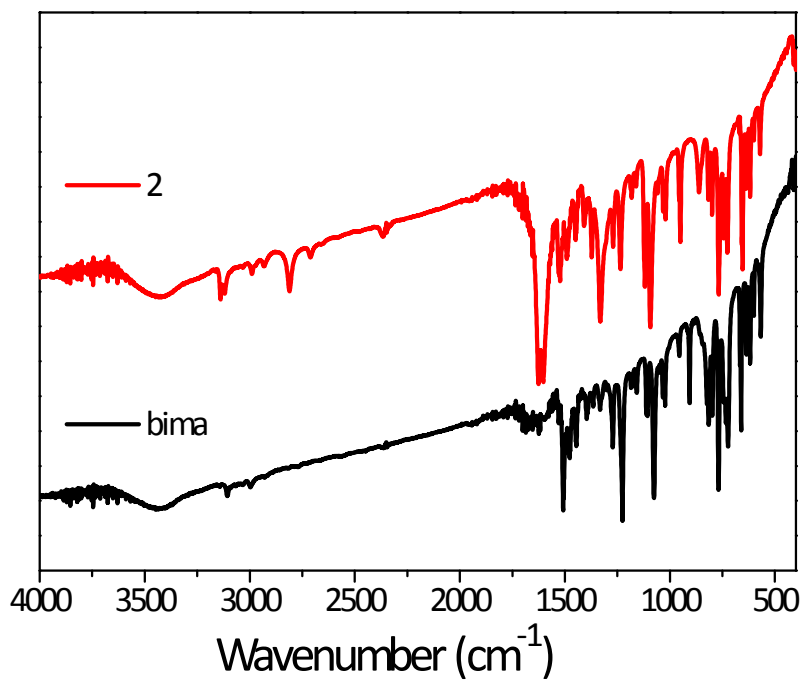
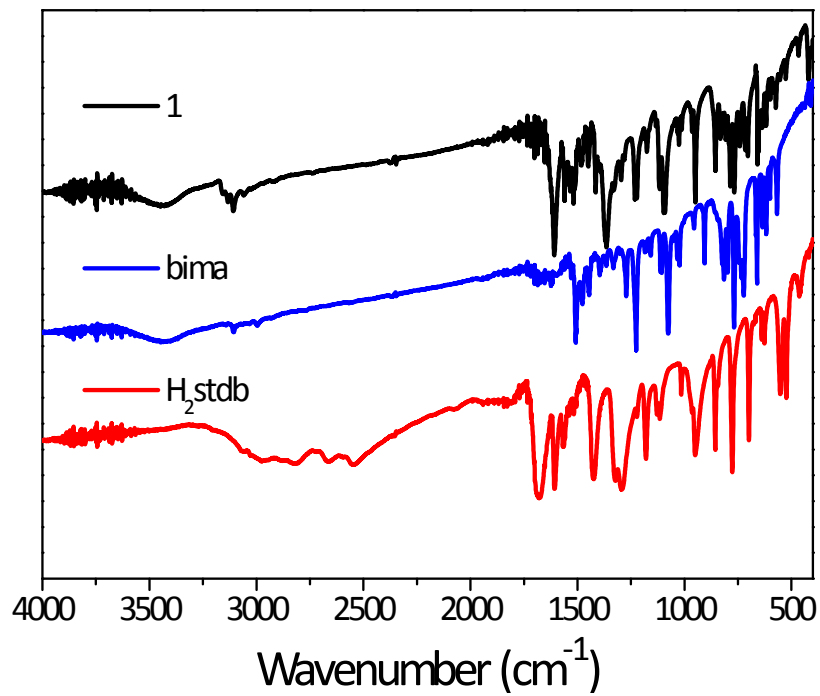


**Fig. S1** FT-IR spectra of ligands, **1** and **2**.

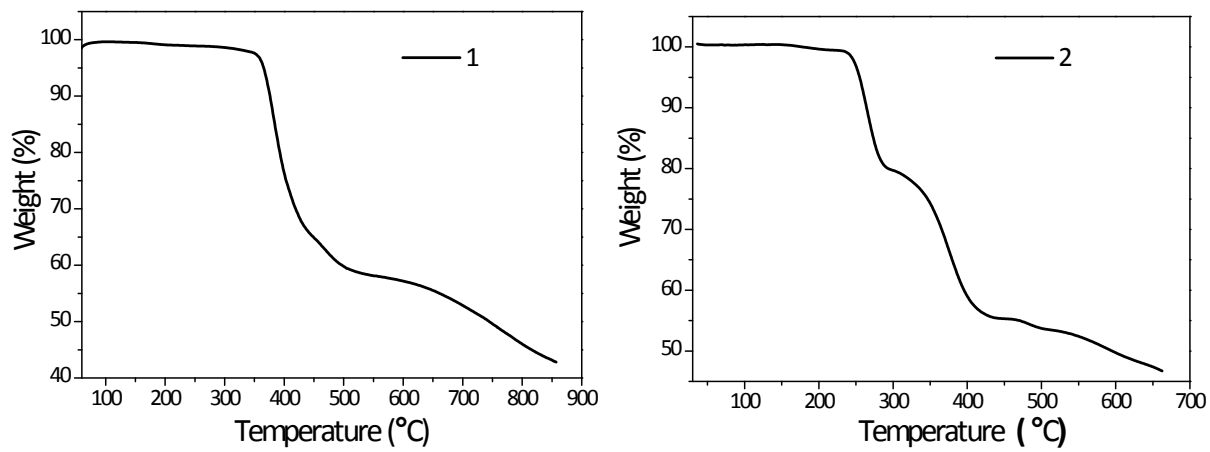


**Fig. S2** Thermogravimetric curves of **1** and **2**.

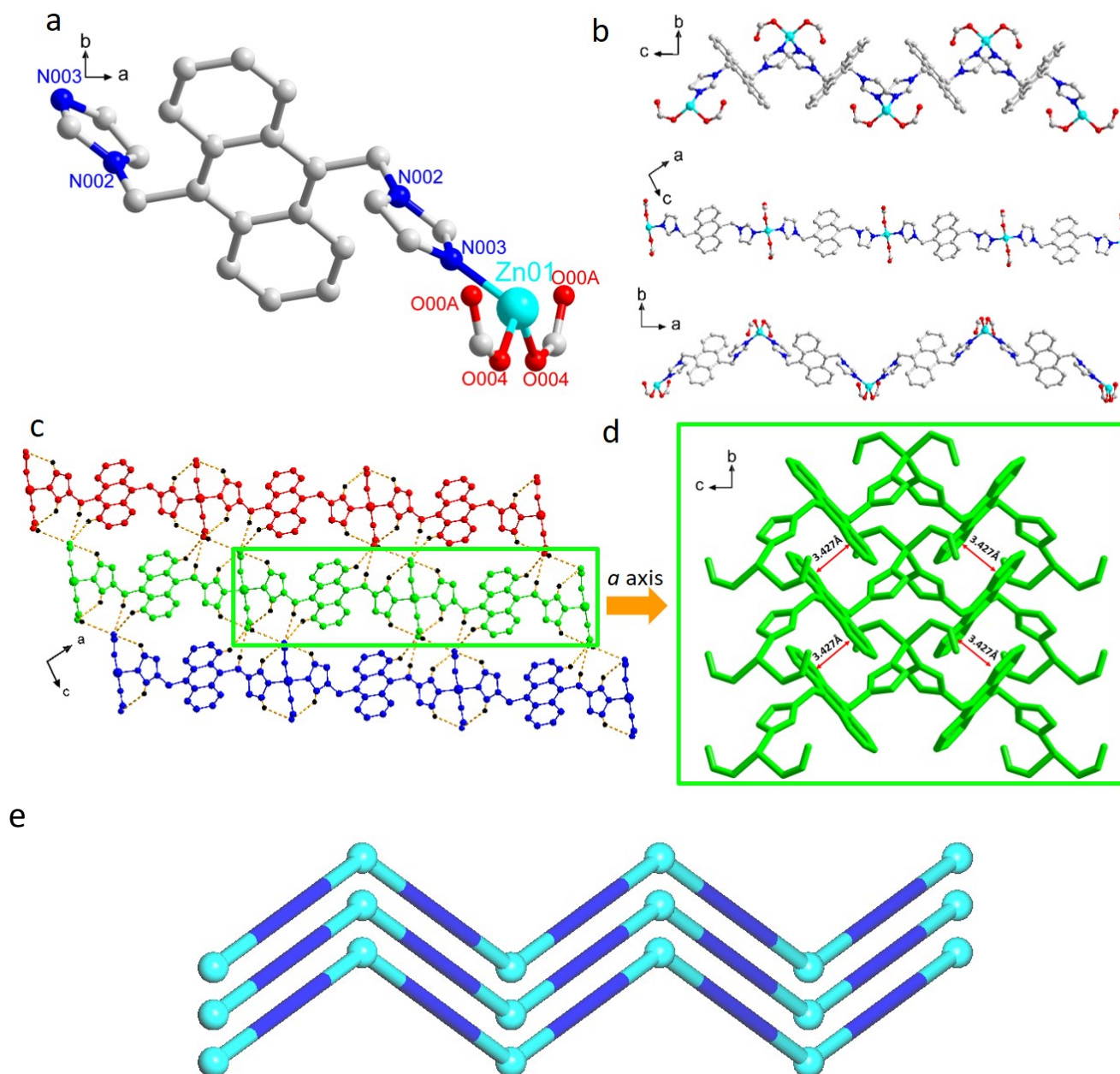


**Fig. S3** A schematic assembly process of **2** and its structural representation. (a) Asymmetric unit (b) 1D coordination polymer chain structure (views along different axis). (c) Fragments of three adjacent 1D chains displayed in different colors that are assembled into a supramolecular network by weak C-H...O hydrogen bonds. (d) Three adjacent interdigitated 1D chains that are interconnected by  $\pi$ - $\pi$  interactions. For clarity, irrelevant H atoms are omitted, color codes: Zn (cyan balls), O (red), N (blue), C (gray), H (black). (e) Topological representation of three adjacent 1D chains with the 2C1 topology; Zn (cyan balls), centroids of  $\mu$ -bima linkers (blue).

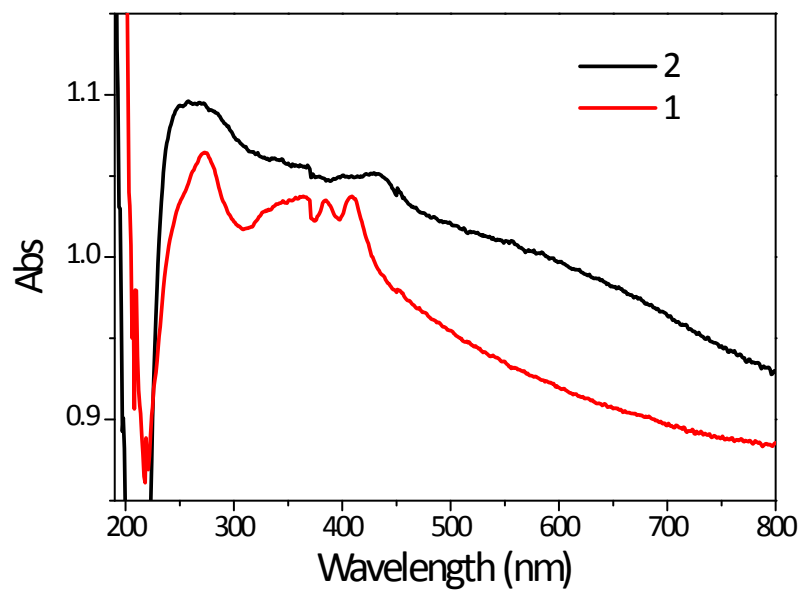


**Fig. S4** Solid-state UV-Vis absorption spectra of **1** and **2**.



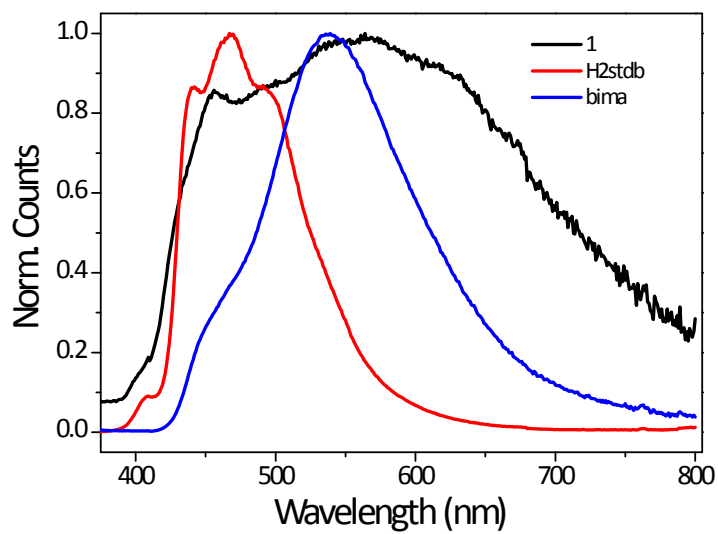


**Fig. S5** Solid-state emission spectra of **1** and organic ligands.

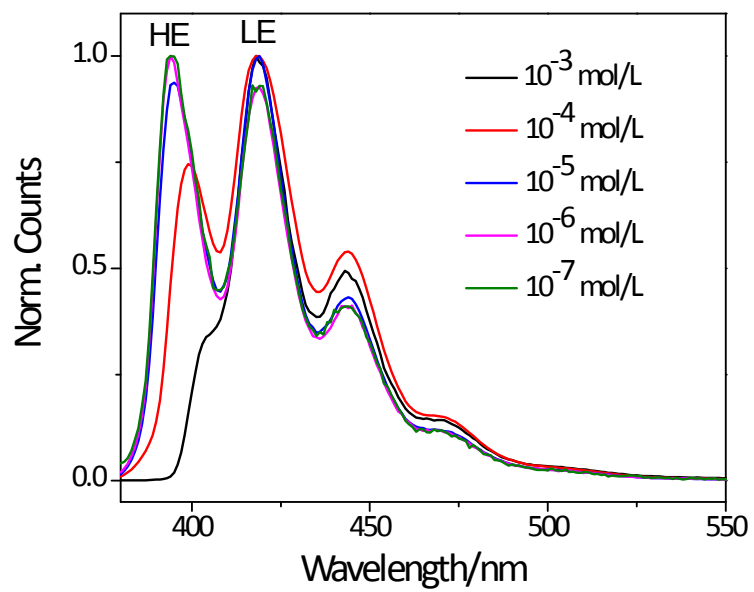


**Fig. S6** Concentration-dependent emission spectra of **bima** ligand in MeOH ( $\lambda_{\text{ex}} = 360$  nm).

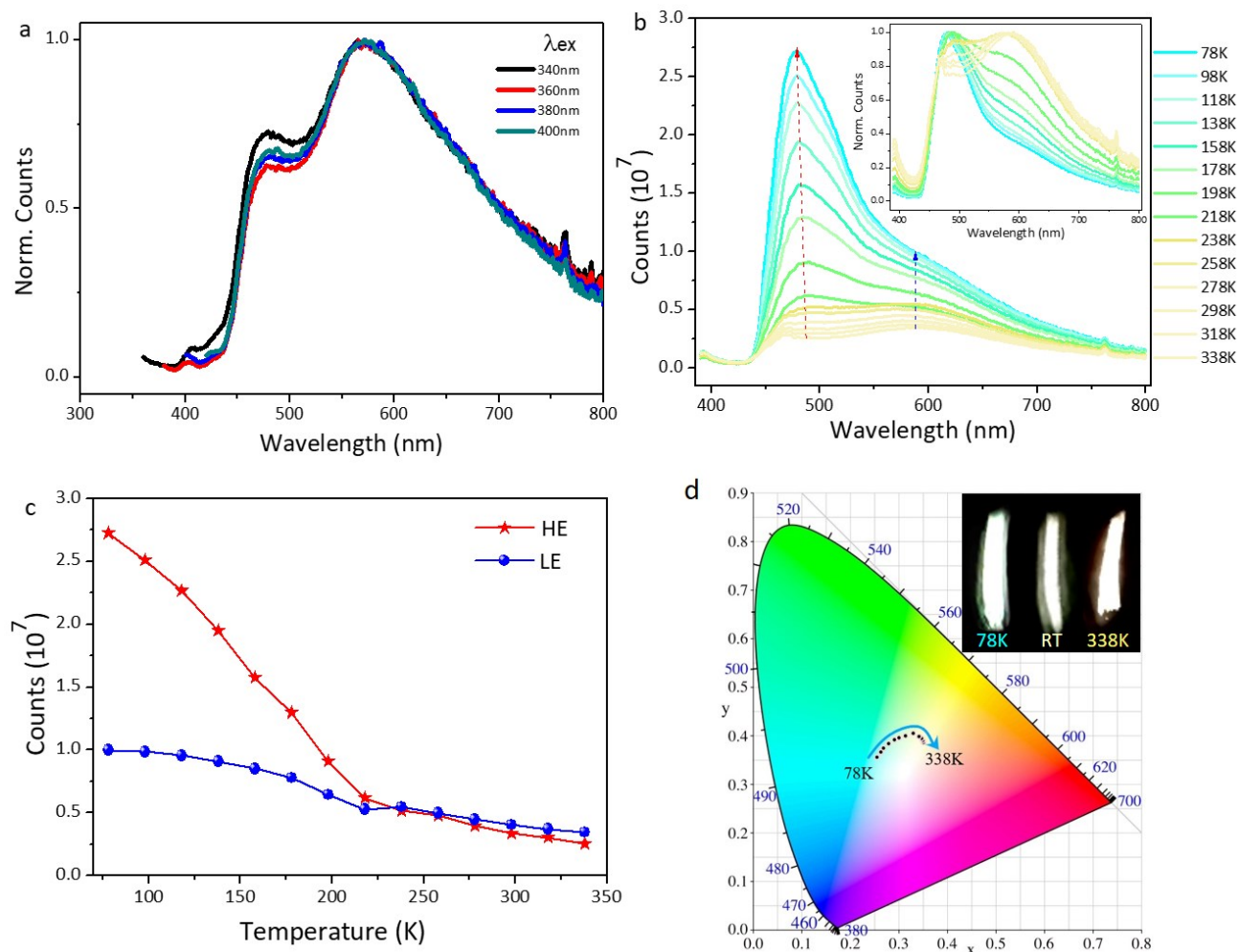


**Fig. S7** (a) Solid-state emission spectra of **2** at different excitation wavelengths at room temperature, (b) Temperature-dependent emission spectra of **2**. (c) Changes in HE and LE of **2** at different temperatures. (d) CIE coordinates of the emission spectrum of **2** at different temperatures.

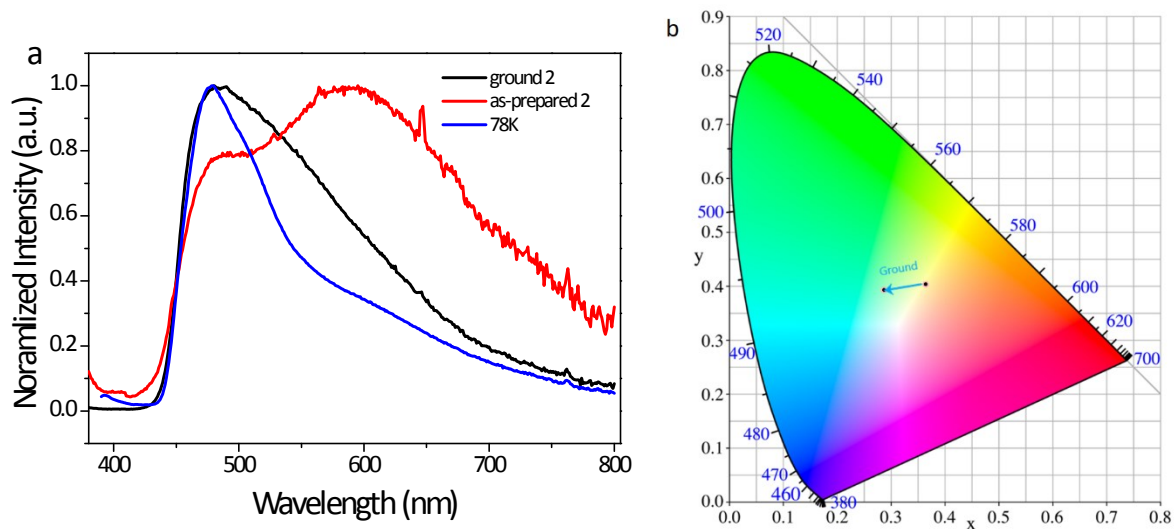


**Fig. S8** Changes in the emission spectra and CIE coordinates of **2** before and after grinding. The quantum yield value of **2** is enhanced from 6.26 to 15.7% due to the mechanical grinding.

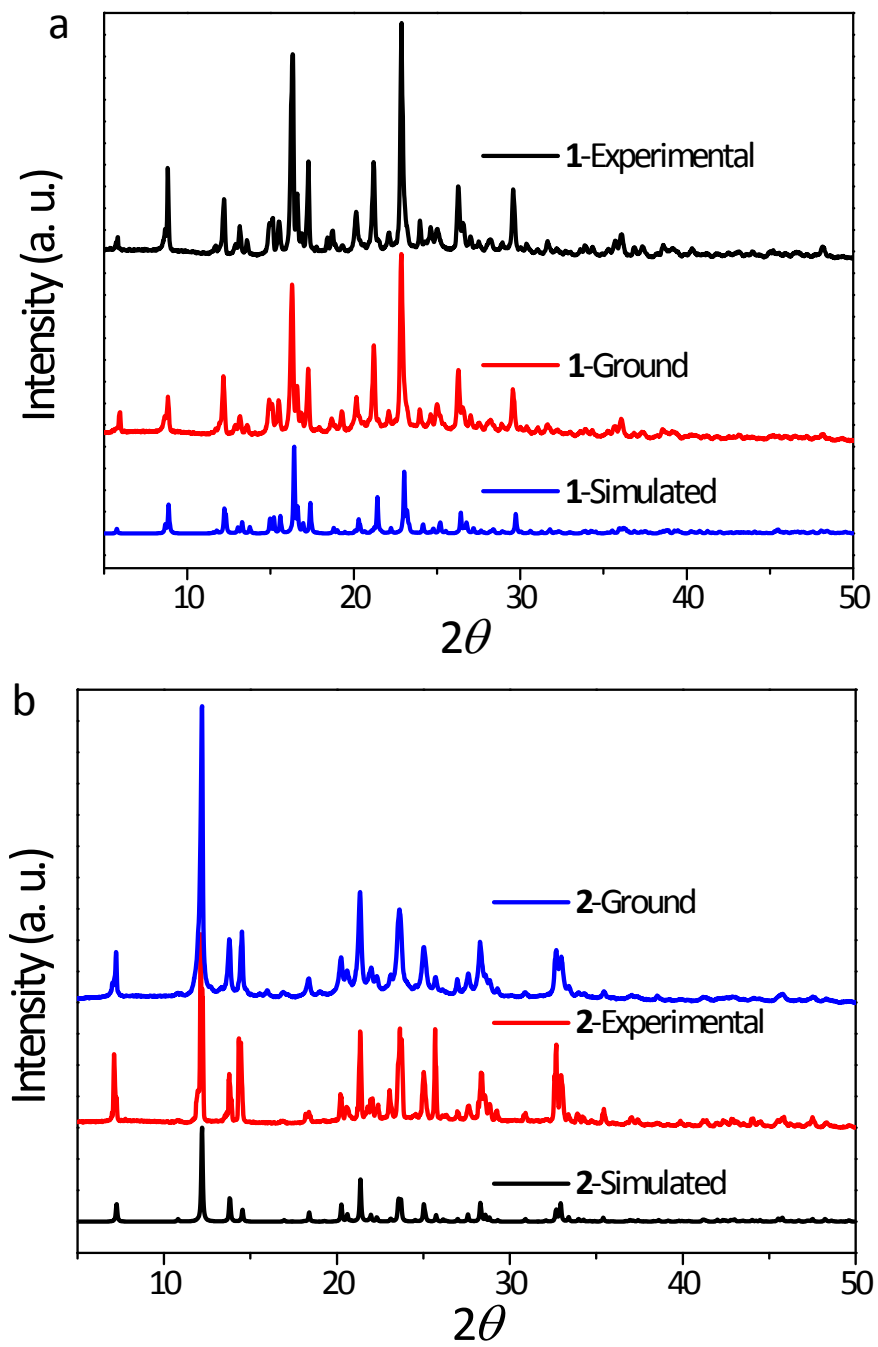


**Fig. S9** Powder X-ray diffraction patterns of **1** (top) and **2** (bottom) before and after grinding.